DOI: 10.61782/fa.2025.0452

FORUM ACUSTICUM EURONOISE 2025

IMPACT OF RESONANCE LOADING ON THE SOUND GENERATION FROM IN-DUCT POINT SOURCES

Maximilian Behn* **Ulf Tapken**
German Aerospace Center, Institute of Propulsion Technology, Engine Acoustics Department
Berlin, Germany

ABSTRACT

Analytical models of the sound generation from ducted turbomachinery stages often apply spatially distributed point sources such as monopoles and dipoles, which can be derived from the in-duct Green's function. Another important application of point source models is the localisation of sound source distributions, which is done inside ducts so far mainly for fan stages. One difficulty with current point source models is the unconstrained excitation of resonant modes at their cut-on frequencies leading to unrealistically high sound power levels. Simultaneously, the resonant modes manifest an immense loading on the point sources according to Newton's third law. To achieve more realistic predictions, an extension of the point source models is developed that accounts for the impact of resonance loading by including an internal source impedance. The resulting sound power distribution over the range of cut-on modes is derived for relevant source configurations and compared with reference models and experimental data from a fan test rig.

Keywords: acoustic point source model, mode excitation, sound power, flow ducts

1. INTRODUCTION

The design and further improvement of turbomachinery stages with low noise excitation relies on accurate prediction tools to support the design process during the pre-design phase. These tools are often semi-analytical, and model the sound generation from the rotor and stator by application of equivalent, spatially distributed point sources [1, 2]. Depending on the sound generating mechanism, the point sources can have monopole, dipole and quadrupole characteristics. Another important application of in-duct point source models is the localisation of source distributions from microphone array measurements [3, 4]. In both fields of application, the reliability of existing tools and methods is impeded at the mode cut-on frequencies, where single modes are resonant, and an infinite mode amplitude and sound power is predicted, which overestimates the resonant mode excitation in comparison with experimental observations. Different approaches have been proposed in the past, ranging from sound power correction terms for the sound power radiated into the far field, as proposed by Moreau [2], to a complete disregard of the resonant mode behaviour, as proposed by Dougherty [5] for the localisation of in-duct noise sources.

In order to provide a physics-based source model that achieves more realistic predictions of the resonant mode excitation, the in-duct point source model of Goldstein [1] is extended by including an internal source impedance. Doak stated that acoustic sources in turbomachinery stages are constrained by an internal source impedance, but did not provide an explicit expression of the form of the source model [6]. So far, the concept of internal source impedance has been applied in ducted systems only for frequencies below the cut-on frequency of the first higher-order modes (e.g. [7–9]). This article describes an extended in-duct point source model for the prediction of the excitation of higher-order, acoustic modes in resonant and off-resonant conditions. The impact of the model extension is evaluated by example of monopole and dipole source distributions and by comparison with experimental results from a fan test rig.

**Corresponding author*: maximilian.behn@dlr.de.

2. POINT SOURCES IN FLOW DUCTS

The sound radiation from a monopole source at position $(\check{x}, \check{r}, \check{\phi})$ in a cylindrical flow duct of radius R is described as a superposition of acoustic modes and can be derived from the in-duct Green's function (see e.g. [1]):

$$p^{\pm}_{\text{monopole}}\left(x, r, \phi|\check{x}, \check{r}, \check{\phi}\right) = q\frac{\rho c}{4\pi R^2}\cdot \sum_{m=-\infty}^{\infty}\sum_{n=0}^{\infty}\frac{f_{mn}(r)f_{mn}(\check{r})}{\alpha_{mn}}e^{im(\phi-\check{\phi})}e^{ik^{\pm}_{mn}(x-\check{x})} \tag{1}$$

with volume flow q as source strength, density ρ and speed of sound c. Each mode is described in terms of the azimuthal order m, radial order n, axial wave number $k^{\pm}_{mn}$ and radial mode shape factor $f_{mn}(r)$, which in combination yield the mode transfer function $f_{mn}(r)e^{i\left(m\phi+k^{\pm}_{mn}x\right)}$ [10]. The generated mode amplitude $A^{\pm}_{mn}$ is proportional to $q\frac{\rho_0 c}{4\pi R^2}\frac{1}{\alpha_{mn}}$, where α_{mn} denotes the mode propagation factor, which ranges between 0 and 1 above the mode cut-on frequency and is imaginary for cut-off modes. As a consequence, the mode amplitude reaches infinite sound pressure at the mode cut-on frequency. In terms of sound power, which is given for cut-on modes by the following expression

$$P^{\pm}_{mn} = \frac{\pi R^2}{\rho c}\frac{\alpha_{mn}(1-M_x^2)^2}{(1\mp\alpha_{mn}M_x)^2}|A^{\pm}_{mn}|^2, \tag{2}$$

The $1/\alpha_{mn}$-term in the expression of the mode amplitude cancels the α_{mn}-term in Eq. (1) resulting in an infinite sound power of resonant modes with $\alpha_{mn} = 0$ excited by a monopole source. Therefore, similarly to the mode amplitude, the mode sound power $P^{\pm}_{mn}$ is proportional to $\frac{1}{\alpha_{mn}}$.

At subsonic operating conditions, the dominant acoustic sources in turbomachinery stages have dipole characteristics [1]. The generated sound pressure from a dipole source is obtained from the directional derivative of the monopole Green's function in Eq. (1) with respect to the dipole axis given by vector $\mathbf{n} = [\cos\alpha_{\text{dipole}};\ 0;\ \sin\alpha_{\text{dipole}}]^T$ [11] [1]:

$$\begin{aligned} p^{\pm}_{\text{dipole}}\left(x, r, \phi|\check{x}, \check{r}, \check{\phi}\right) &= \partial_{\mathbf{n}} p^{\pm}_{\text{monopole}}\left(x, r, \phi|\check{x}, \check{r}, \check{\phi}\right) \\ &= \nabla p^{\pm}_{\text{monopole}}\cdot\mathbf{n} \\ &= q_d\frac{\rho c}{4\pi R^2}\cdot \end{aligned} \tag{3}$$

$$\sum_{m=-\infty}^{\infty}\sum_{n=0}^{\infty} -i\left(k^{\pm}_{mn}\cos\alpha_{\text{dipole}} + \frac{m}{\check{r}}\sin\alpha_{\text{dipole}}\right)\cdot \frac{f_{mn}(r)f_{mn}(\check{r})}{\alpha_{mn}}e^{im(\phi-\check{\phi})}e^{ik^{\pm}_{mn}(x-\check{x})} \tag{4}$$

with dipole moment q_d. Note, that the gradient ∇ is evaluated with respect to the source position $(\check{x}, \check{r}, \check{\phi})$. Equation (4) shows that the mode amplitude and, hence, the mode sound power have generally the same proportionality with $\frac{1}{\alpha_{mn}}$ as for the monopole source. Only for $M_x = 0$, the $\frac{1}{\alpha_{mn}}$-term is lifted for modes with azimuthal mode order $m = 0$.

3. MODEL EXTENSION BY SOURCE IMPEDANCE

The infinite sound power output from in-duct point sources at the mode cut-on frequencies stands in contradiction to two experimental observations of the excited sound field from turbomachinery stages. Firstly, an increased sound pressure is indeed measured at the mode cut-on frequencies, typically at low frequencies, but it does not reach infinite amplitudes. Therefore, according to Eq. (4) with $\alpha_{mn} = 0$ the resulting, measured mode sound power is zero in contrast to the analytical model, which predicts an infinite sound power. Secondly, towards higher frequencies the density of mode cut-on frequencies increases exponentially, which leads to a high number of resonance peaks in the analytically modelled spectra, but measured sound pressure spectra do not show any resonance effects in this frequency range.

In comparison, the sound power output from a point source in free field conditions increases monotonously with [12]

$$P = \frac{k^2\rho c}{8\pi}q^2 \tag{5}$$

for a monopole source, respectively

$$P = \frac{k^4\rho c}{12\pi}q_d^2 \tag{6}$$

[1] The assumption that the dipole axis lies in the x-ϕ-plane is valid for blades with sufficiently small lean.

for a dipole source. It appears plausible that a point source in a duct at high characteristic frequencies kR should generate a sound power output at a similar level to that in free field conditions. Albeit, the point source model in Eq. (1) predicts much higher sound power levels, in particular for modes near their cut-on frequencies. In the following, the in-duct point source model of a monopole source is extended in order to achieve a more realistic characteristics of the sound power output. The transfer to dipole sources is easily made using Eq. (3).

The mode impedance $Z^{\pm}_{mn} = A^{\pm}_{mn}/q$ is chosen as the starting point for the model extension. More precisely, it is given by the following expression:

$$Z^{\pm}_{mn}\left(\check{x},\check{r},\check{\phi}\right) = \frac{\rho c}{4\pi R^2}\frac{f_{mn}(\check{r})}{\alpha_{mn}} e^{-im\check{\phi}} e^{-ik^{\pm}_{mn}\check{x}}. \quad (7)$$

The mode impedance describes the ratio of the excited mode amplitude to the source volume flow. However, it can also be interpreted as the pressure on the source as a back reaction of the mode relative to the source strength [6]. At the mode cut-on frequencies the pressure of the resonant modes becomes infinite. In the idealised point source models in Eq. (1) and (4) the back reaction of the modes on the source is not considered, so that the source effectively acts as a constant volume flow source. Morfey [13] investigated the behaviour of this source type as well as constant pressure sources and showed that in the latter case no resonance phenomena occur. A more realistic source model, whose behaviour lies somewhere between these two extremes, is obtained by including an internal source impedance for each cut-on mode. An illustration of the extended model is given in Fig. 1.

The model is based on an electroacoustic analogy, which considers the volume flow q as current and pressure resp. mode amplitude as voltage. It is assumed that the loading due to each mode does not depend on the source position. Therefore, the factors of the mode impedance in Eq. (7) that are independent from the source position are separated from the position-dependent terms, i.e. $\hat{Z}^{\pm}_{mn} = \frac{\rho c}{4\pi R^2}\frac{1}{\alpha_{mn}}$. The model's network structure allows a straightforward analysis employing Kirchhoff's loop and node laws. For each mode, the mode impedance is connected in parallel with the internal source impedance resulting in the effective mode impedance of the internal source impedance (ISI-)model given by:

$$\hat{Z}^{\pm}_{mn,\mathrm{ISI}} = \frac{Z_S \cdot \hat{Z}^{\pm}_{mn}}{Z_S + \hat{Z}^{\pm}_{mn}}. \quad (8)$$

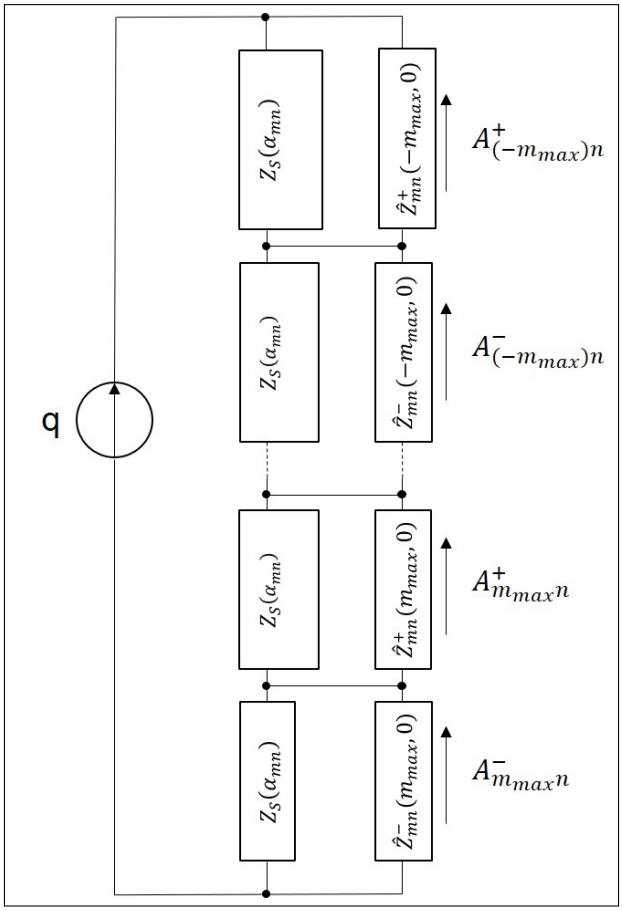

Figure 1. Illustration of the extended source model with internal source impedance Z_S and radiation impedances $Z^{\pm}_{mn}$.

In combination with the source position-dependent terms, the excited mode amplitude according to the ISI-model is expressed as:

$$Z^{\pm}_{mn,\mathrm{ISI}} = \frac{A^{\pm}_{mn}}{q} = \hat{Z}^{\pm}_{mn,\mathrm{ISI}} f_{mn}(\check{r}) e^{-im\check{\phi}} e^{-ik^{\pm}_{mn}\check{x}}. \quad (9)$$

At the mode cut-on frequencies, the loading due to $Z^{\pm}_{mn}$ is very high, so that the effective mode impedance of the ISI-model yields:

$$Z^{\pm}_{mn,\mathrm{ISI}}\left(\alpha_{mn}=0\right) \approx Z_S. \quad (10)$$

Thus, modes are not excited with infinite pressure at their cut-on frequencies, but instead the mode amplitude yields $A^{\pm}_{mn}\Big|_{\alpha_{mn}=0} = Z_S q$.

Additional fundamental assumptions are:

1. each mode is an additional load for the source,
2. the source impedance relates the in-duct source output to the free field case, and
3. the influence of the source impedance is maximal for resonant modes and diminishes for $\alpha_{mn} \to 1$.

A natural choice for the internal source impedance of an in-duct monopole source is the radiation impedance of a monopole source in free field conditions, which is given by [12]:

$$Z_{FF} = \frac{p_{FF}}{q} = \frac{\rho c}{4\pi R^2} (kR)^2 . \tag{11}$$

However, Z_{FF} shows a low sound pressure excitation at low frequencies. In order to achieve a realistic resonance behaviour at low frequencies, an additional term $\chi(kR)$ is included that increases the mode excitation at low frequencies. Finally, the first and last assumptions lead to the following expression of the internal source impedance:

$$\begin{aligned} Z_S(\alpha_{mn}) =& \frac{Z_{FF} + \chi(kR)}{N_M \cdot (1 - \alpha_{mn})} \\ =& \frac{\rho c}{4\pi R^2} \frac{(kR)^2 + \frac{25}{kR}}{N_M \cdot (1 - \alpha_{mn})}. \end{aligned} \tag{12}$$

with the number of cut-on modes N_M. The expression of the additional term $\chi(kR)$ is hypothetical and primarily included to demonstrate the behaviour of the proposed model extension. The low-frequency characteristics of the internal source impedance requires further investigation.

The internal source impedance in Eq. (12) distributes the sound generation potential according to the free field radiation impedance over all cut-on modes by division by the number of cut-on modes N_M. The additional term $1/(1 - \alpha_{mn})$ corresponds to the third fundamental assumption. This choice increases the impact of resonance loading on the excitation of modes, which are close to their cut-on frequencies, while modes with a high propagation factor, i.e. $\alpha_{mn} \to 1$, are not affected by resonance loading. As a result, the internal source impedance Z_S approaches infinity for modes with a high propagation factor, which means that for these modes the ISI point source model acts a constant volume flow source.

The effective mode impedance in Eq. (9) yields after some rearrangement:

$$Z^{\pm}_{mn,\mathrm{ISI}} = \frac{Z^{\pm}_{mn}\left(\check{x}, \check{r}, \check{\phi}\right)}{1 + \frac{N_M}{(kR)^2 + \frac{25}{kR}} \frac{1 - \alpha_{mn}}{\alpha_{mn}}}. \tag{13}$$

4. EVALUATION OF SOURCE DISTRIBUTIONS USING THE EXTENDED SOURCE MODEL

The extended source model is evaluated for dense distributions of two different source types:

- incoherent monopoles and
- incoherent dipoles with $\alpha_{\mathrm{dipole}} = -\frac{\pi}{4}$,

which are distributed equally over the duct cross-section.

As an example, the duct geometry and flow conditions of DLR's fan test rig CRAFT (Co-/Counter-Rotating Acoustic Fan Test Rig) are considered. The duct diameter is 453.6 mm. The flow Mach number in the inlet is $M_x = 0.11$ at the fan design point. Further information is provided in [14].

Figure 2 shows the development of the internal source impedance as a function of the non-dimensional frequency kR for $\alpha_{mn} = 0$. The internal source impedance approaches an asymptotic limit of approximately 2 already at relatively low frequencies. Between $kR = 5$ and 25, the normalised internal source impedance is almost constant and predominantly determined by Z_{FF}/N_M. The results show that the additional term $\chi(kR)$ has an impact only at low frequencies $kR < 5$.

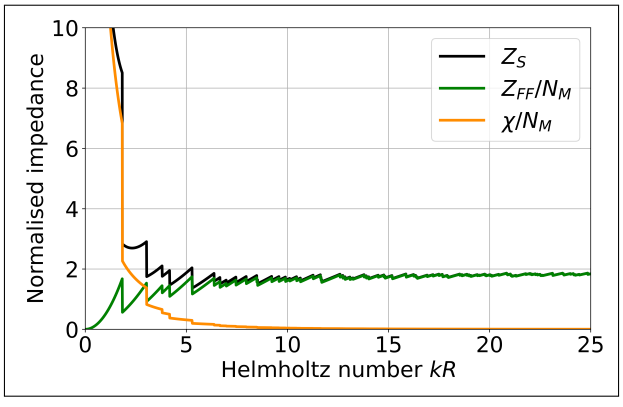

Figure 2. Internal source impedance Z_S and its components as a function of non-dimensional frequency. Values are normalised by $\frac{\rho c}{4\pi R^2}$.

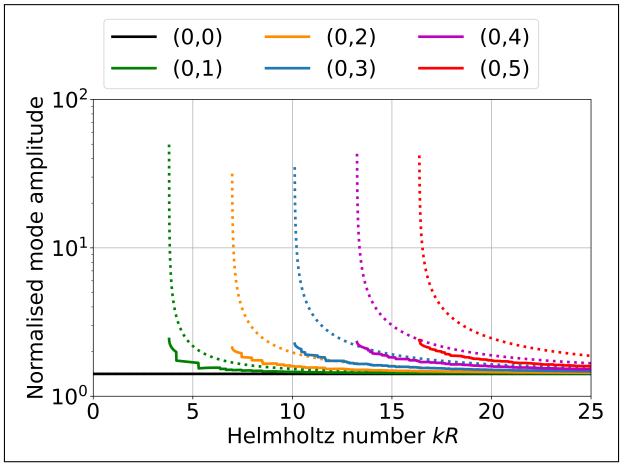

Figure 3. Mode amplitudes for azimuthal mode order $m = 0$ excited by a dense distribution of incoherent monopole sources. Values are normalised by $\frac{\rho c}{4\pi R^2}$. Solid lines show results for the ISI-model and dashed lines for the Goldstein point source model.

The mode amplitudes with azimuthal mode order $m = 0$ that are excited by the distribution of monopole sources, are displayed in Fig. 3. The plane wave mode $(0, 0)$ has a propagation factor $\alpha_{00} = 1$ and therefore, is not affected by resonance loading. All higher radial mode orders exhibit significantly lower amplitudes close to the cut-on frequencies in comparison to the reference point source model by Goldstein (cp. Eq. (1)). The mode amplitude of mode $(0, 1)$ is characterised by two larger discontinuities, which occur due to a discrete increase of N_M at neighbouring mode cut-on frequencies. With increasing frequency, the cut-on of additional mode orders has a small impact on the mode amplitude curves, because the number of cut-on modes N_M is growing exponentially. Furthermore, both point source models converge asymptotically towards high frequencies. However, whereas for mode $(0, 1)$ the predicted mode amplitudes are almost equal within $\Delta kR = 5$ to 6 from the mode cut-on frequency, the convergence of the predicted mode amplitudes extends over a much larger frequency range for higher radial mode orders. For example, for mode $(0, 4)$ convergence is observed for approximately $\Delta kR = 10$. Thus, the impact of resonance loading is stronger towards high frequencies.

The most important characteristics of the newly proposed ISI-model is observed from the development

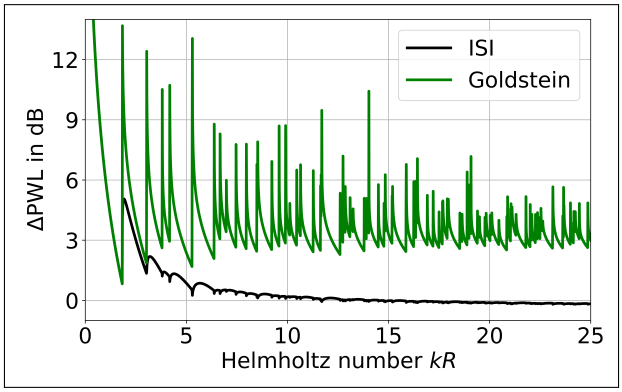

Figure 4. Total sound power generated by a dense distribution of incoherent monopole sources relative to the sound power output of a monopole source in free field conditions (cp. Eq. (5)).

of the total sound power, which is depicted in Fig. 4. At low frequencies, both source models show significantly increasing sound power levels at the mode cut-on frequencies, but the levels of the ISI-model are limited with e.g. an increase of 4 dB at the cut-on frequency of the modes $(\pm 1, 0)$ compared to more than 11 dB for the Goldstein point source model. Towards high frequencies, the ISI-model approaches the sound power level of the free field source asymptotically, while the results of the Goldstein model exhibit strongly fluctuating sound power levels and an average offset of approximately 2.5 dB.

The second source distribution consists of dipole sources, whose dipole axes are oriented at -45 degrees with respect to the duct axis. The excited mode amplitudes of azimuthal mode order $m = 0$ are presented in Fig. 5 and the total sound power in Fig. 6.

The trend of the mode amplitude curves for the distribution of dipole sources is almost inverted to those for the monopole distribution. The results for the reference model indicate a very narrow notch of the mode amplitude curves near to the cut-on frequencies and an asymptotic increase towards high frequencies. The impact of the ISI-model is twofold. Firstly, the maximum mode amplitude at the cut-on frequency is strongly reduced. And secondly, the rate of increase is reduced, which is particularly pronounced with increasing radial mode order. Both characteristics of the ISI-model can also be identified in Fig. 6. Due to the limitation of the

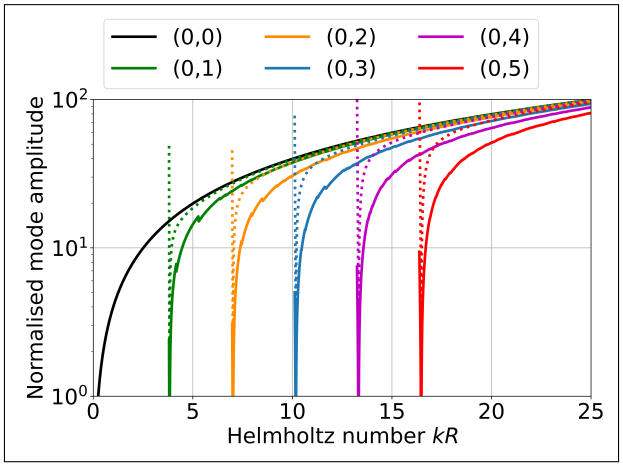

Figure 5. Mode amplitudes for azimuthal mode order $m = 0$ excited by a dense distribution of incoherent dipole sources. Values are normalised by $\frac{\rho c}{4\pi R^2}$. Solid lines show results for the ISI-model and dashed lines for the Goldstein point source model.

maximum mode amplitude at the cut-on frequencies, the total sound power exhibits a smooth development with respect to frequency above $kR = 5$ in contrast to the results of the Goldstein point source model. Furthermore, the general rate of increase of the sound power predicted by each model is similar to that of the free field dipole source. An offset of approximately 2.5 dB for both source models is reached at $kR = 25$, which is similar to the monopole case. Note, however, that the difference between the ISI-model and the free field dipole does not indicate a less accurate prediction, because, unlike in the free field, the sound power output of the ducted dipole sources is influenced by the dipole angle with respect to the duct axis.

5. COMPARISON WITH EXPERIMENTAL RESULTS

In this section, the sound power distributions obtained with the Goldstein and the ISI point source models are compared with experimentally determined mode sound powers using radial mode analysis. The details of the measurements on the CRAFT test rig and the analysis of the measurement data are given in [15].

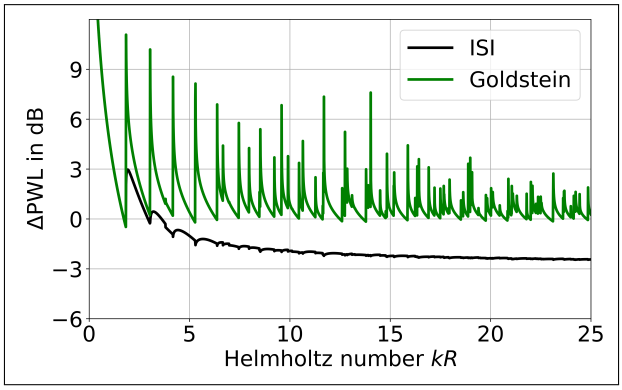

Figure 6. Total sound power generated by a dense distribution of incoherent dipole sources relative to the sound power output of a dipole source in free field conditions (cp. Eq. (6)).

Figures 7 and 8 show the mode sound power distribution of the rotor-incoherent, broadband sound field component at $kR \approx 20$, which were measured in the inlet and outlet of the CRAFT at the aerodynamic design point of the fan stage. In the inlet, only upstream propagating and rotor co-rotating modes are considered for the comparison, because the rotor shielding effect has an additional effect on the sound power distribution that is not included in the modelling discussed here. In contrast, in the outlet only downstream propagating, rotor counter-rotating modes considered. Additionally, modelled mode sound power distributions according to distributions of dipole sources with $\alpha_{\text{dipole}} = -\frac{\pi}{4}$ using the Goldstein and the ISI point source models as well as two mode energy distribution models: "'equal mode energy"' (EME) and "'equal mode energy density"' (EDEM), which are matched to the total measured sound power.

The modelling results show two different trends. On the one hand, the "'equal mode energy"' distribution corresponds to a constant sound power level independent of the mode propagation factor. Interestingly, the results of the Goldstein point source model show a trend that is similar to the EME distribution. On the other hand, the "'equal mode energy density"' predicts an increasing sound power level for high values of the mode propagation factor. A very similar trend is observed for the ISI point source model.

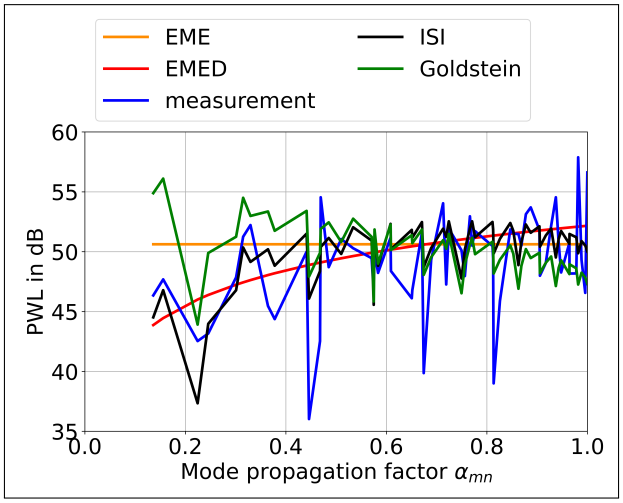

Figure 7. Comparison of measured mode sound power in the inlet of the CRAFT test rig and matched distributions from different source and mode energy distribution models at $kR \approx 20$.

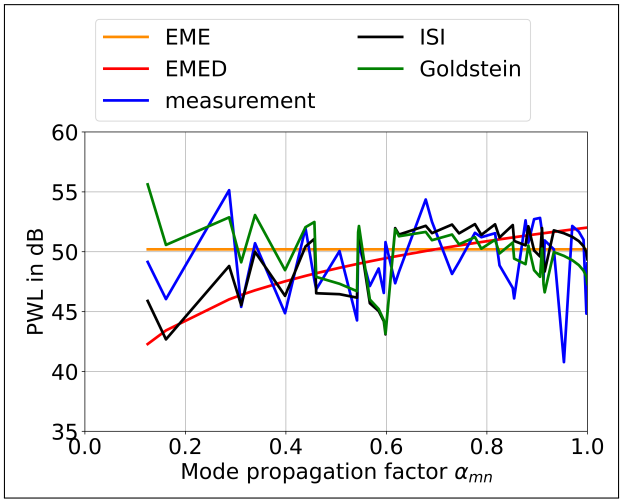

Figure 8. Comparison of measured mode sound power in the outlet of the CRAFT test rig and matched distributions from different source and mode energy distribution models at $kR \approx 20$.

In comparison with the measured sound power distribution, the EMED distribution and the prediction using the ISI-model achieve a very good agreement in the inlet regarding the overall trend. In case of the ISI-model, the distribution of dipole sources at a single axial plane is insufficient in order to predict dips in the mode sound power distribution like the ones at $\alpha \approx 0.45$, 0.67 and 0.81, which correspond to the modes $(-1, 3)$, $(-1, 4)$ and $(-1, 5)$.

In the outlet, the results of the ISI-model are in good agreement with the measured sound power levels above $\alpha = 0.3$. For modes that are closer to their cut-on frequencies, the measured sound power levels are elevated, which is caused by resonant excitation of the modes, but also by stronger reflections at the rotor of the corresponding modes $(18, 0)$, $(13, 1)$ and $(9, 2)$.

6. CONCLUSION

The widely used point source models by Goldstein are extended by incorporation of an internal source impedance (ISI) with the aim to achieve a more realistic excitation of acoustic modes in resonant conditions. For the internal source impedance, the radiation impedance of a monopole point source in free field conditions is taken in combination with an additional term, that boosts the mode excitation at low frequencies. The evaluation of monopole and dipole distributions demonstrates the effective reduction of overestimated mode sound powers at the cut-on frequencies leading to a continuous total sound power spectrum above $kR = 10$. A good agreement of the predicted sound power distribution using the ISI-model is found in comparison with experimental data from DLR's CRAFT fan test rig. Furthermore, the trend of the sound power distribution from the ISI-model resembles the "'equal mode energy density"' (EMED) distribution in contrast to the original Goldstein model, which shows a stronger resemblance to the "'equal mode energy"' model (EME). The demonstrated characteristics of the ISI-point source model are particularly beneficial for the robustness of noise prediction tools and source localisation techniques for turbomachinery stages, especially, at high frequencies, where the modal density increases exponentially.

7. ACKNOWLEDGMENTS

The authors are grateful for the support of Lukas Klähn and Wolfram Köhler in providing the experimental data from the CRAFT test rig.

This research has been performed in the frame of the project COMPANION (COMmon Platform and

Advanced iNstrumentration readIness for ultra efficient propulsiON), which is funded by the European Union Clean Aviation Joint Undertaking program, under grant agreement No. 101140627.

CLEAN AVIATION Co-funded by the European Union

8. REFERENCES

[1] M. E. Goldstein, *Aeroacoustics*. New York: McGraw-Hill International, 1976.

[2] A. Moreau, *A unified analytical approach for the acoustic conceptual design of fans of modern aero-engines*. Dissertation, Technical University Berlin, Berlin, Germany, 2017.

[3] C. R. Lowis, *In-duct measurement techniques for the characterisation of broadband aeroengine noise*. Dissertation, University of Southampton, Southampton, UK, 2008.

[4] H. Brouwer and P. Sijtsma, "Phased array beamforming to identify broadband noise sources in the interstage section of a turbofan engine," in *25th AIAA/CEAS Aeroacoustics Conference*, (Delft, Netherlands), May 2019.

[5] R. P. Dougherty and J. M. Mendoza, "Nacelle in-duct beamforming using modal steering vectors," in *14th AIAA/CEAS Aeroacoustics Conference*, (Vancouver, Canada), May 2008. 10.2514/6.2008-2812.

[6] P. E. Doak, "Excitation, transmission and radiation of sound from source distributions in hard-walled ducts of finite length (i): The effects of duct cross-section geometry and source distribution space-time pattern," *Journal of Sound and Vibration*, vol. 31, pp. 1–72, 1973.

[7] P. K. Baade, "Effects of acoustic loading on axial flow fan noise generation," *Noise Control Engineering Journal*, vol. 8, pp. 5–15, 1977.

[8] M. G. Prasad, "A four load method for evaluation of acoustical source impedance in a duct," *Journal of Sound and Vibration*, vol. 114, pp. 347–356, 1987.

[9] H. Bodén, "The multiple load method for measuring the source characteristics of time-variant sources," *Journal of Sound and Vibration*, vol. 148, pp. 437–453, 1991.

[10] U. Tapken, *Analyse und Synthese akustischer Interaktionsmoden von Turbomaschinen*. Dissertation, Technical University Berlin, Berlin, Germany, 2016.

[11] E. Williams, *Fourier Acoustics*. London: Academic Press, 1999.

[12] K. U. Ingard, *Fundamentals of waves and oscillations*. Cambridge: Cambridge University Press, 1988.

[13] C. L. Morfey, "Rotating pressure patterns in ducts: Their generation and transmission," *Journal of Sound and Vibration*, vol. 1, pp. 60–87, 1964.

[14] U. Tapken, L. Caldas, R. Meyer, M. Behn, L. Klähn, R. Jaron, and A. Rudolphi, "Fan test rig for detailed investigation of noise generation mechanisms due to inflow disturbances," in *AIAA AVIATION 2021 FORUM*, (virtual), August 2021.

[15] L. Klähn, R. Meyer, and U. Tapken, "Inflow distortion noise and turbulence measurements in a low speed fan test rig," in *30th AIAA/CEAS Aeroacoustics Conference*, (Rome, Italy), June 2024.